Bioorganic & Medicinal Chemistry xxx (2012) xxx–xxx

Contents lists available at SciVerse ScienceDirect

Bioorganic & Medicinal Chemistry

journal homepage: www.elsevier.com/locate/bmc

Natural products as a gold mine for selective matrix metalloproteinases inhibitors

Liyan Wang [a,†], Xi Li [a,†], Shoude Zhang [b,†], Weiqiang Lu [a], Sha Liao [a], Xiaofeng Liu [a], Lei Shan [c], Xu Shen [a], Hualiang Jiang [a], Weidong Zhang [b,c,*], Jin Huang [a,*], Honglin Li [a,*]

[a] *Shanghai Key Laboratory of New Drug Design, State Key Laboratory of Bioreactor Engineering, School of Pharmacy, East China University of Science and Technology, Shanghai 200237, China*
[b] *School of Pharmacy, Shanghai Jiao Tong University, Shanghai 200240, China*
[c] *Department of Phytochemistry, School of Pharmacy, Second Military Medical University, Shanghai 200433, China*

ARTICLE INFO

Article history:
Received 18 February 2012
Revised 17 April 2012
Accepted 18 April 2012
Available online xxxx

Keywords:
Matrix metalloproteinases
Virtual screening
Natural product
Anticancer agent

ABSTRACT

Nineteen natural compounds with diverse structures are identified as potential MMPIs using structure-based virtual screening from 4000 natural products. Hydroxycinnamic acid or analogs of natural products are important for potent inhibitory and selectivity against MMPs, and the solvent effect in the S1′ pocket can affect the hydrophobic interactions and hydrogen bonds between MMPIs and MMPS, making MMPIs exhibit certain selectivity for a specific MMP isoenzyme. Furthermore, compound **5** can reduce the expression of both MMP-2 and active-MMP-9, and suppress the migration of MDA-MB-231 tumor cell in a wound healing assay, which may be further developed as an anticancer agent.

1. Introduction

Matrix metalloproteinases (MMPs) are a group of zinc dependent proteolytic enzymes able to cleave all major protein components of the extracellular matrix (ECM: collagen, laminin, firbronectin, etc.) as well as a number of bioactive mediators (growth-factor-binding proteins, cellsurface receptors, cell-adhesion molecules, precursors of other proteinases, etc.).[1,2] Over the past 30 years, MMPs have been considered as attractive cancer targets and a lot of different types of synthetic inhibitors have been identified as anticancer drugs.[3] But only a few of small MMPs inhibitors (MMPIs) have been undergoing clinic trials, some trials were prematurely terminated due to either lack of benefits or major adverse effects and failed to reach their expectations of increasing survival.[4] One possibility is drugs were only performed in patients with advanced stage tumors because the studies in animal models had shown that MMPIs would be more active in early stages of tumor.[5] Second possibility is the MMPIs used in clinical trials were broad-spectrum drugs that also inhibited the MMP's anti-tumor effects and influenced MMPs mediation of normal physiological processes.[6] The third possible reason may be that most synthetic MMPIs have high toxicity, the minimum effect does is close to the toxic response does that cause toxic response or adverse reactions.[7] Therefore, more selective and more new skeleton MMPIs devoid of adverse reactions which are detected with broad-spectrum inhibitors are needed to treat cancer.

The disappointing results of synthetic MMPIs in human clinical trial make the intense need for compounds more effective in cancer treatment and this search found its answer in the field of natural compounds.[8] Natural products are an important source of novel leads for drugs discovery, and were recognized as a rich source for finding novel lead structures that are active against a series of drug targets.[9] For example, Neovastat® (isolated from *Shark cartilage*) was reported to have inhibited enzymatic activity of MMP-2 with minor inhibition of MMP-1,-7,-9 and -13,[8] and it is in phase II trial in patients suffering from multiple myeloma as well as in nonsmall cell lung cancer and in renal cell carcinoma.[10–12] *Genistein*, which is an isoflavonoid of the leguminosae family and mainly found in soy products, also inhibits invasion in human breast carcinoma cell lines by diminishing the expression of MMP-2, -9.[13] Since collecting all the bioactive natural products and screening them randomly is unpractical for its laborious and time-consuming characters, the problem is how to select the natural products from microbial, plant, marine or other sources for their MMPs inhibition assay in vitro and in vivo. To solve the problem, virtual screening becomes a reliable, inexpensive method for identifying natural leads.[14]

* Corresponding authors. Tel./fax: +86 21 64250213.
E-mail addresses: wdzhangy@hotmail.com (W. Zhang), huangjin@ecust.edu.cn (J. Huang), hlli@ecust.edu.cn (H. Li).
† These authors contributed equally to this work.

0968-0896/$ - see front matter © 2012 Elsevier Ltd. All rights reserved.
http://dx.doi.org/10.1016/j.bmc.2012.04.063

In recent years, virtual screening has become an important part of the drug discovery process.[14] Compared to high-throughout screening, structure-based virtual screening coupled with structural biology is promising to increase the success rate of various projects in the lead identification stage of the drug discovery process.[15] Although structure-based virtual screening has led to the development of compounds in clinic trials or on the market, its application has so far almost been neglected for the discovery of lead structures from natural products.[15–17]

In all MMPs family members, the gelatinase sub-family, gelatinase A (MMP-2) and gelatinase B (MMP-9), have been implicated in a number of pathological events leading to cancer, inflammatory diseases, cardiovascular diseases, and neurological disorders.[18] Here we report a successful structure-based virtual screening for novel potential MMP-9 inhibitors from an in-house Natural Product Database (NPD), which is a collection of 4000 natural products isolated from 100 medicinal plants by our group. Corresponding inhibitory activities against other MMPs (MMP-1, MMP-2, MMP-

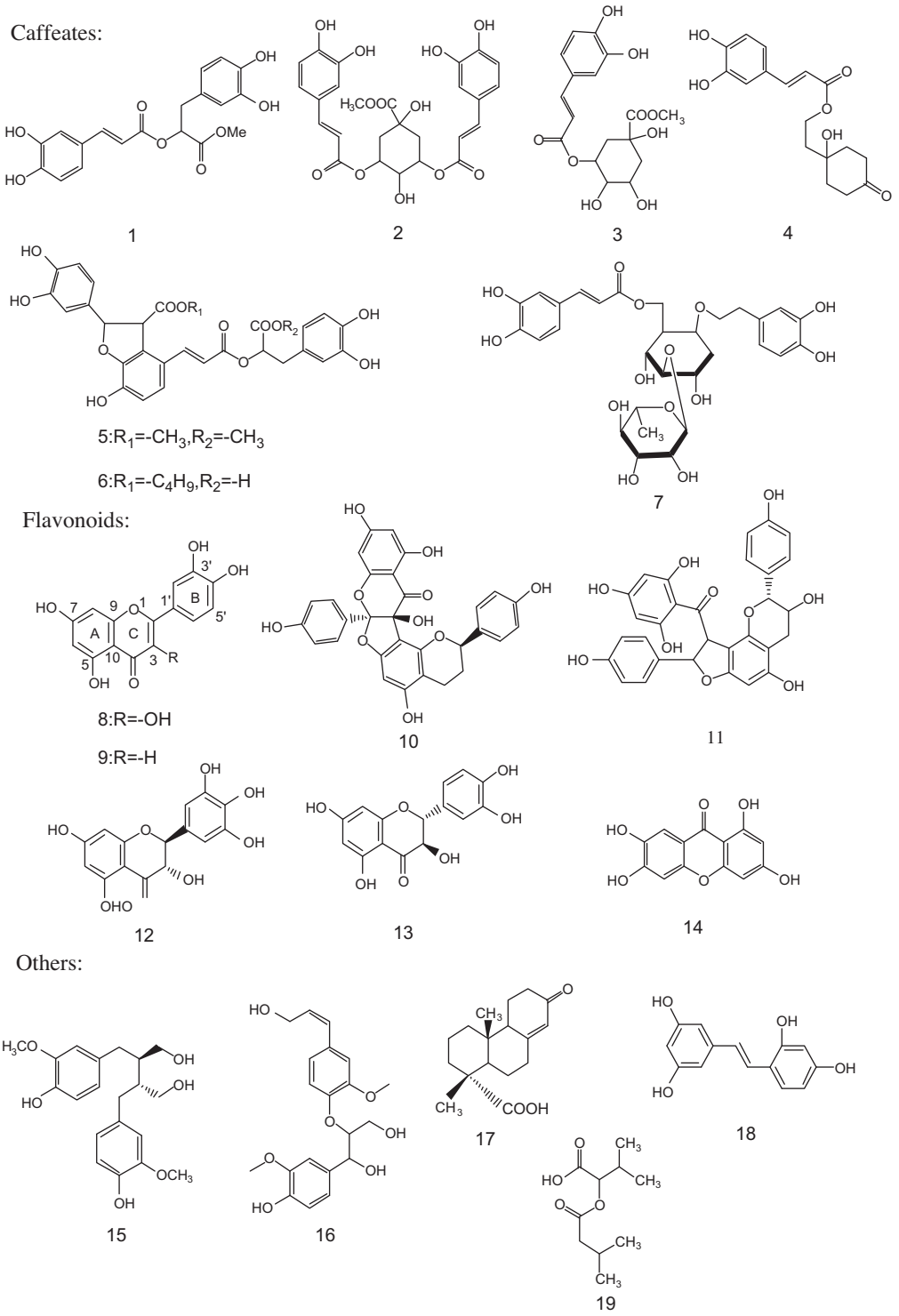

Figure 1. Structures of the natural compounds.

3 MMP-12 and MMP-13) isoenzymes as well as potential binding poses of the hit compounds are also reported.

2. Results and discussions

Nineteen natural compounds are identified to exhibit inhibitory activities against MMPs through virtual screening and the biological test. The hit compounds can be divided into three classes according to their structures: caffeates, flavonoids and others (Fig. 1). The inhibitory activities against MMPs iosenzymes are listed in Table 1. Most of the caffeates exhibit more potent inhibitory activities and selectivities against MMP-9 than other MMPs, such as compounds **1** and **5**, which exhibit potent inhibition against MMP-9 with IC_{50}s of 0.61 and 0.99 μM, respectively. On the contrary, the flavonoids show poorer activity and selectivity against MMP-9 than that of the caffeates. Other compounds have no inhibitory activity against most of MMPs, except MMP-9 and MMP-2 with micromolar-level inhibitory activities. In order to investigate the selectivity and activities of these compounds for different MMPs, the binding modes of the caffeate compound **5** and flavonoid compound **8** are proposed by the molecular docking simulation (Fig. 2).

2.1. Predicting the binding modes of inhibitors with MMP-9

The active site of MMPs is divided into six sub-sites of S3–S3′, which are composed of amino acid residues that interact with the physiological substrates, natural and synthetic inhibitors.[19] According to the predicted binding pose (Fig. 2A), as is commonly observed among known inhibitors of MMPs, a carbonyl group of the α,β-unsaturated ketone in the central saddle for the caffeate compound **5**, forms a chelate bond with the catalytic zinc ion of the enzyme. Near the zinc ion, the polar oxygen of the ester in the linker moiety interacts with the side chain of Gln402 by hydrogen bond. We also find that the ligand can occupy two sub-pockets (S1′ and S3) of MMP-9 with good intermolecular contacts. In the S1′ sub-pocket, the ligand's terminal aryl ring makes hydrophobic contacts with several hydrophobic residues, such as Met422 and His401. In addition, the hydroxyl of the terminal aryl ring is predicted to form hydrogen bond with the polar atoms of residues Leu397. Meanwhile, similar interactions are observed in the S3 sub-pocket: Pro421 forms hydrophobic interaction with the other aryl ring of the ligand, and the hydroxyls of the terminal aryl ring form hydrogen bonds with the polar atoms of Tyr420.

Compared with the caffeate compounds, those flavonoid inhibitors show lower potencies for MMPs. According to the predicted binding pose of compound **8** (Fig. 2**B**), flavonoid inhibitors also share the same key pharmacophoric characters as caffeate inhibitors, making flavonoid inhibitors exhibit moderate inhibition against MMPs. Compound **8** also deeply binds in the S1′ pocket of MMP9, the B-ring of **8** forms hydrophobic contacts with Leu397, Tyr423, Met422 and His401; the 4-carbonyl group exhibits weak chelation with zinc cation, and 3- and 4′- hydroxyl groups form hydrogen bonds with Gln402 and Leu397, respectively. However, compared with compound **5**, compound **8** lacks some important functional groups, such as catechol group and dihydrobenzofuran group which occupied the S3 pocket, and more hydrophobic interactions and hydrogen bonds with the amino residues in this region are not observed. Due to the lack of pharmacophoric characters as above mentioned, other compounds exhibit poorer inhibitory activities against MMP-9 and other MMPs.

2.2. The possible reasons for the selectivity against different MMPs

MMPs are homologous enzymes, and their sequence similarities and identities are in the range from 50% to 88% and from 33% to 79%, respectively.[20] There is a common sequence motif HExGHxxGxxH in the active site, where the three histidine residues coordinate the catalytic zinc ion. Moreover, the tertiary structures of all MMPs typically share three α-helices and five β-sheets consisting of four parallel and one anti-parallel.

Although all MMPs are homologous and have high similarity sequences, some small differences can still be found according to the information from the sequence. The sequence alignment for six dif-

Table 1
Inhibition activities of natural compounds against six MMPs

Compounds	IC_{50}[a] (μM)					
	MMP-1	MMP-2	MMP-3	MMP-9	MMP-12	MMP-13
1	14.74	3.58	28.26	0.61	2.75	29.03
2	16.32	3.88	10.36	11.61	1.2	7.62
3	ND[b]	64.19	58.81	ND	ND	ND
4	ND	ND	ND	12.49	ND	ND
5	8.23	11.65	8.15	0.99	0.67	18.52
6	3.25	15.47	14.81	3.46	1.79	24.49
7	ND	8.96	91.41	14.28	8.22	11.09
8	ND	6.68	5.57	1.61	10.23	8.46
9	ND	3.61	16.2	5.62	0.98	10.05
10	ND	23.28	22.3	21.24	ND	13.17
11	ND	14.11	25.55	10.17	ND	43.55
12	ND	11.9	20.27	28.79	1.74	9.33
13	ND	22.62	33.91	32.02	5.75	34.6
14	11.36	ND	ND	ND	ND	ND
15	50.12	ND	ND	ND	ND	ND
16	ND	ND	ND	9.91	ND	ND
17	ND	33.26	ND	ND	ND	ND
18	ND	27.6	ND	ND	ND	ND
19	10.56	23.32	38.15	14.28	ND	42.52
MMP inhibitor II	ND	ND	0.0286	0.0018	ND	ND
MMP inhibitor III	0.0041	0.0036	ND	ND	0.0082	0.0064

[a] The IC_{50} was made if the inhibition rate was more than 30% at the concentration of 10 μM. The IC_{50} values were determined from the results of at least three independent tests of MMPs activity.
[b] Not determined.

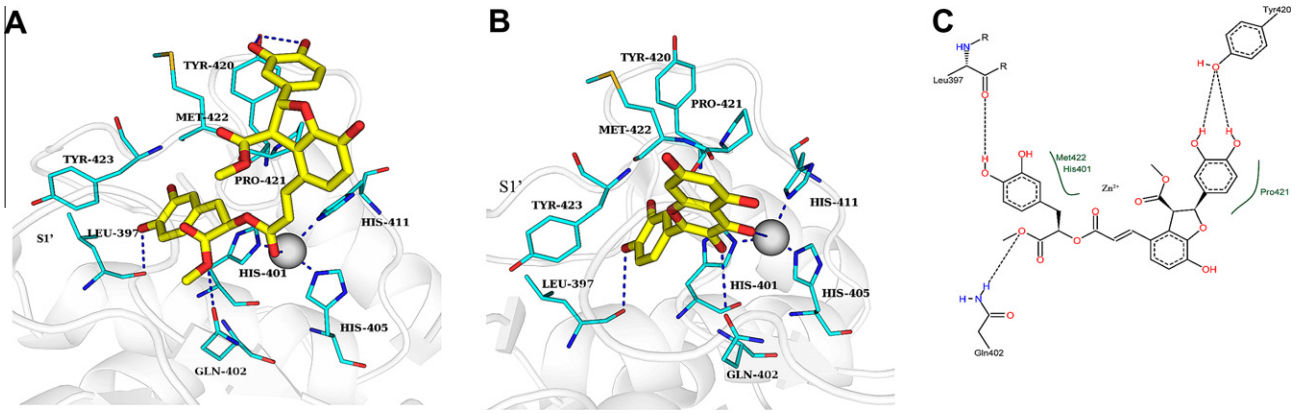

Figure 2. The predicted binding mode of compound **5** (A) and compound **8** (B) in the binding site of MMP-9 (PDB code 1GKD). Residues in contacts with the ligand are illustrated with lines; carbon atoms are colored in cyan, nitrogen atoms in blue, sulfur atoms in yellow and oxygen atoms in red; the activity zinc ion is illustrated with gray sphere; hydrogen bonds are represented by dotted blue lines. The predicted pose of compound **5** and **8** are shown in yellow stick. In the 2D depiction of ligand-protein interaction in (C), inter-molecular hydrogen bonds are represented by dashed lines, and hydrophobic effect is represented by green lines. (A) and (B) were drawn through the Pymol[24] and (C) was through the PoseView[25] (http://poseview.zbh.uni-hamburg.de/).

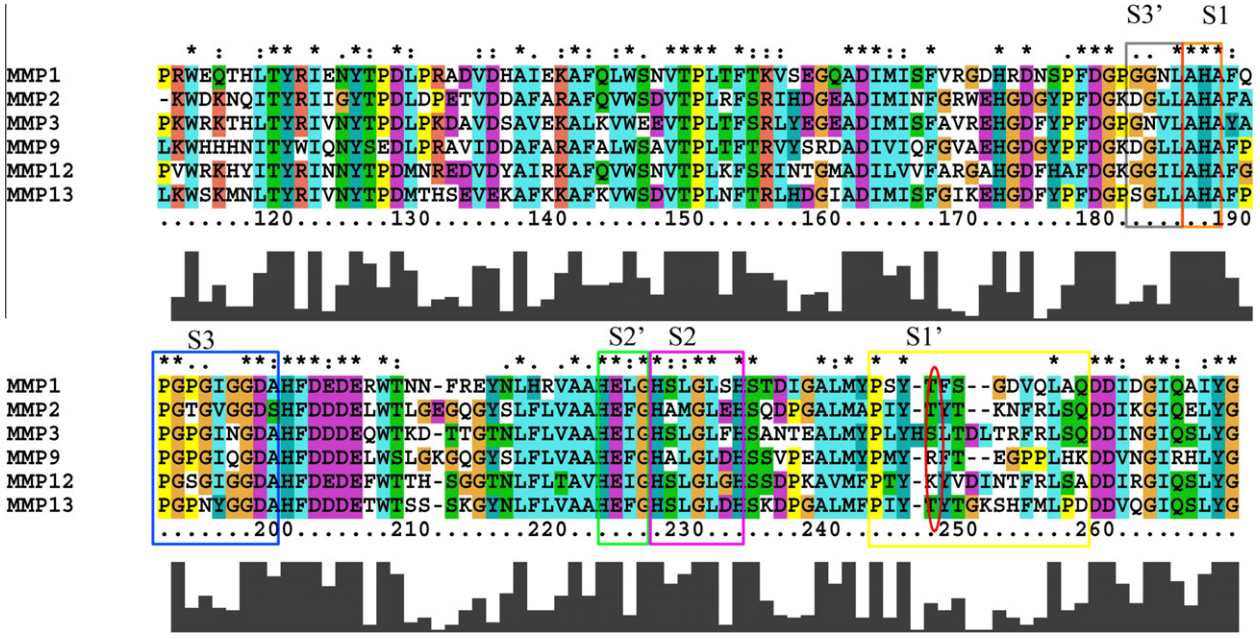

Figure 3. Sequences alignment for the catalytic domain of six MMPs structures, the degrees of the shading and the histogram correlate the amino acid similarity. The amino acid sequences were retrieved from the SWISS-PROT protein sequence data bank: MMP-1 (entry P03956), MMP-2 (entry P08253), MMP-3 (entry P08254), MMP-9 (entry P14780), MMP-12 (entry P39900) and MMP-13 (entry P45452). The sequence alignment was performed using the program ClustlaX 2.0, and revised by minor manual adjustments. The rectangle frames in different colors indicated the sequences of the different subpockets. The red ellipse frame indicated the position 245 (MMP-13 numbering).

ferent MMPs (Fig. 3) show that the S1′ pockets are more obvious with different length and amino acid composition to each other. So this sub-pocket is considered as an important inhibitor-protein interaction region as well as a prominent site of intervention for obtaining selectivity.[20–22]

Further exploitation of the differences of MMPs in the S1′ pocket revealed that the S1′ pocket is surrounded by a loop, and the flexible loop and the amino acid sequence variability influence the shape and size of S1's pocket of all the MMPs, which critically determine MMP selectivity. From our result, the MMPs used in this study generally fall into two classes in terms of the S1′ pocket: MMP-1 has smaller and closed pocket, while MMP-2, -3, -9, -12 and -13 have much larger pockets. This is undoubtedly related to the fact that the MMP-1's relatively small S1′ pocket restricts the compounds which are filled up with a large hydrophobic group. As expected, 12 out of all 19 inhibitors are not potent against MMP-1.

The S1′ pockets of MMP-9, -12 are almost as large as that of MMP-2, -3, -13, but we found that at position 245 (MMP-13 numbering), the amino acid residues are different from each other (Fig. 3). The arginine and lysine with longer side chain locate in MMP-9 and MMP-12, respectively, and the neutral serine and threonine with hydroxide group locate in the MMP-2, MMP-3 and MMP-13. Superposition of the position 245 amino residue (MMP-13 numbering) of MMP-2, MMP-9 and MMP-12, respectively (Fig. 4), clearly shows that the Lys241 in MMP-12 and Arg424 in MMP-9 covering the pocket partly, turns into the bottom of the

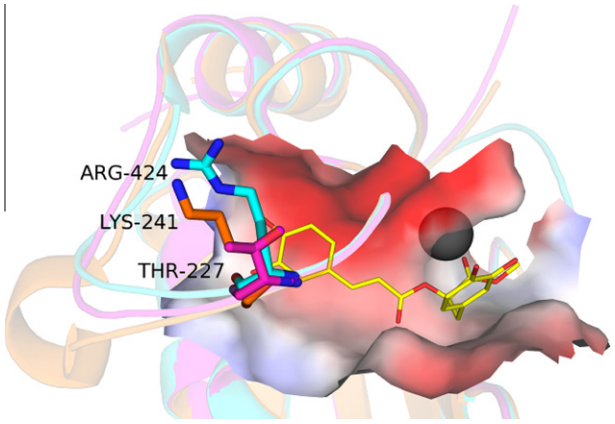

Figure 4. Superposition of Thr227 (magenta) of MMP-2 (1QIB) and Lys241(orange) of MMP-12 (1ROS) on Arg424 (cyan) of MMP-9 (1GKD). The predicted binding mode of the compound **1** is represented by the yellow lines.

S1′ pocket's tunnel, but in MMP-2 the residue is replaced by threonine with shorter side chain. The residues of MMP-3 and -13 at this position, like MMP-2, also have short side chains, which almost did not cover the S1′ pocket. Results indicate that the degree of the solvent exposure for different enzymes is different in the S1′ pocket. Meanwhile as we discussed in the predicted binding modes of the compounds, there are important hydrophobic interactions and hydrogen bonds in the S1′ pocket to make the natural product specifically bind with the enzyme. It is presumed that due to the different degree of the solvent exposure in the S1′ pocket, the solvation effect is different for the binding ligand among different MMPs enzymes. Since solvation effect can decrease the potential hydrogen bonds and hydrophobic interactions between ligand and enzymes to some extent, the binding affinities of the ligands in the more open S1′ pockets such as MMP-2, -3 and -13 are weaker. As mentioned above, we presumed the difference at position 245 (MMP-13 numbering) might be an important factor leading to the selectivity for MMPs. The solvation effect in the more open S1′ pockets of MMP-2, -3 and -13 might make the ligand's binding force weaker than in the relatively close S1′s pockets of MMP-9 and -12.

2.3. Repressing MMPs expression and suppressing cancer cell migration

Many natural products are reported to not only inhibit the MMPs enzyme activities, but also repress the MMPs expression in cells. To determine whether active compounds repress MMPs expression, compound **5** is selected to evaluate the MMP-2 and MMP-9 expression in cancer cell MDA-MB-231. MDA-MB-231 cells are incubated with 20 ng/ml TPA and 50 μM compound **5** for 24 h, and then the cells were lysed for western blot assay. Two well-characterized MMPs (MMP-2 and MMP-9) are immunoblotted with anti- MMP-2 and anti- MMP-9 protein antibody, respectively, using GADPH as the control. As in Figure 5, the results show that compound **5** possesses strong inhibitory effect on the expression of MMP-2 and active-MMP-9 at the concentration of 50 μM. However, compound **5** has obsolete inhibition effect on the expression of pro-MMP-9. In this concentration, compound **5** has little effect on cancer cell MDA-MB-231 proliferation (data not shown). Collectively, compound **5** not only inhibits MMPs, but also represses MMP-2 and active-MMP-9 expression in MDA-MB-231 cancer cell.

Matrix metalloproteinases are a group of proteolytic enzymes, which are necessary for cancer cell migration and invasion. To investigate whether our active compounds suppress cancer cell migration, compound **5** is chosen for a wound healing assay.

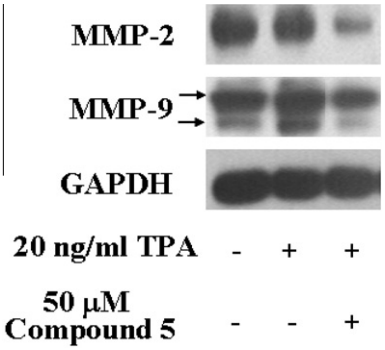

Figure 5. Compound **5** surpressed MMP2 and active-MMP-9 expression in MDA-MB-231cell. The upper arrow is pro-MMP-9 and the lower arrow is active-MMP-9.

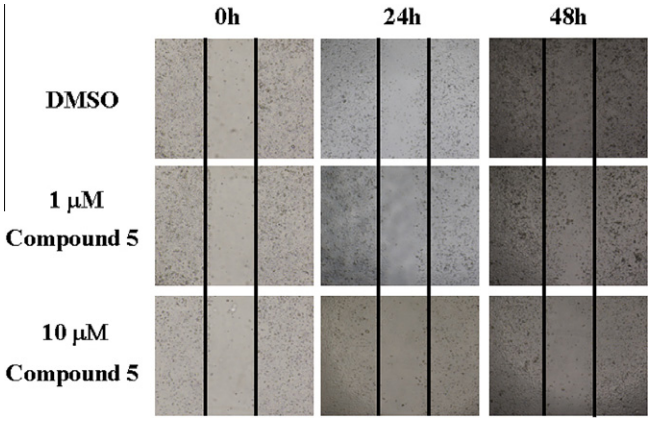

Figure 6. Compound **5** suppressed the migration of MDA-MB-231 cancer cell. Cells were scratched and then treated with 1 and 10 μM compound **5** for 48 h.

MDA-MB-231 is scratched and cells are treated with varied concentration of compound **5** for 48 h. As in Figure 6, compound **5** efficiently suppresses the wound-healing migration of MDA-MB-231 cancer cells at 10 μM concentration, which is endowed with potential utility as the corresponding therapeutic agents for treating cancer cell migration and invasion.

3. Conclusion

In this paper, three key findings emerge from our study: First, 19 natural compounds are discovered as MMPs inhibitors by using structure-based screening and in vitro biologically assay. These compounds have diverse structures and differ from well-known general peptidomimetic and non-peptide hydroxamate inhibitors. Second, SAR and selectivity trends among six different MMPs are also selected to compare the protein sequences and crystal structures. We find that the hydroxycinnamic acid moiety, the common structure in our natural compounds, can generate many key interactions which make the compounds specifically bind with MMPs enzymes. In addition, through the analysis of the overlaid MMP structures, we do see that the shape and size of the S1′ pocket may be the crucial factors for determining the selectivity of MMP inhibitors. Third, compound **5**, the most potent inhibitor in MMPs enzymic assay, also represses the MMP-2 and active-MMP-9 expression in MDA-MB-231 cancer cell and suppresses the migration of MDA-MB-231 in a wound healing assay. A hit-to-lead compound structure optimization based on the compound **5** is undertaken. We believe that the active natural compounds discovered in this study can provide novel scaffolds for more potent and highly selective inhibitors against MMPs.

Please cite this article in press as: Wang, L.; et al. *Bioorg. Med. Chem.* (2012), http://dx.doi.org/10.1016/j.bmc.2012.04.063

4. Experimental section

4.1. Molecular docking

The crystal structure of MMP-9 was retrieved from the Protein Data Bank (PDB entry: 1GKC), and all water molecules were removed from the complex structure. Hydrogen atoms and charges were added during a brief relaxation performed using the 'Protein Preparation Wizard' workflow in Maestro 9.0. After optimizing the hydrogen bond network, the crystal structure was minimized using OPLS 2005 force field with the maximum RMSD value of 0.3 Å. The grid-enclosing box was centered on the ligand in the refined crystal structure as described above and defined so as to enclose residues located within 14 Å from the ligand, and a scaling factor of 1.0 was set to van der Waals (VDW) radii with the partial atomic charges of 0.25 to soften the nonpolar parts of the receptor. And the three-dimensional structures of compounds in the natural product database containing about 4000 molecules were generated with Ligprep module. In the virtual screening process, standard precision (SP) and extra precision (XP) approaches were adopted successively, and 1000 compounds were reserved after being screened with SP mode. Then the top 200 compounds were retrieved and ranked by GlideScore with the XP mode, while these hits were visually inspected for their binding modes. Finally, 60 compounds were selected for the enzyme inhibition against MMP-9 and other MMPs.

4.2. In vitro MMPs inhibition assay

The catalytic domains of recombinant human MMPs (MMP-1, MMP-2, MMP-3, MMP-9, MMP-12, and MMP-13) were prepared in house. The protease activity of MMPs was measured according to the reported method.[23] MMPs activity assays were performed in 96-well half-area plates in a total assay volume of 100 μl. The diluted recombinant MMPs were incubated for 20 min at room temperature in reaction buffer (50 mM Tris–HCl, 150 mM NaCl, 5 mM CaCl2, 0.05% Brij-35, pH 7.5) with different concentrations of the compounds to be tested. For MMP-2, 10 μM ZnCl2 was added to the reaction buffer, and substituted 50 mM MOPS for Tris–HCl. Compounds solutions were prepared from stock in DMSO. After 20 min incubation at room temperature, the substrate was added to a final concentration of 5 μM. Fluorescence intensities (Ex/Em = 340/440 nm) was monitored for 30 min at room temperature with a Synergy™2 Multi-Mode Microplate Reader (BioTek USA). IC_{50} values were calculated by using the GraphPad Prism software with three independent determinations. Positive compound MMP inhibitor II (catalog number 444247) and MMP inhibitor III (catalog number 444264) were obtained from Merck.

4.3. Western blot

For western blot assay, the cells were incubated with 50 μM compound 5 and 20 ng/mL TPA for 24 h. Cells were washed with ice-cold PBS and lysed in buffer containing 20 mM Tris (pH 7.5), 150 mM NaCl, 1% Triton X-100, 1 mM PMSF, supplemented with protease inhibitors (Sigma). The cell lysates were centrifuged at 10000*g* for 10 min at 4 °C, resolved by 10% SDS–PAGE and then transferred to a PVDF membrane (Millipore). After the transfer, the membrane was blocked in TBST buffer with 5% skim milk at 4 °C for overnight. Blots were washed three times in TBS with 0.01% Tween 20 and subsequently incubated with indicated primary antibody horseradish-peroxidase-conjugated secondary antibody in TBS/T buffer. Immunoreactive bands were visualized and quantified using ECL plus™ reagent (GE). The anti-MMP-2, anti-MMP-9 and anti-GAPDH antibody were purchased from Bioworld. Secondary antibodies were obtained from Jackson immunoResearch.

4.4. Wound healing assay

The migration of MDA-MB-231 cancer cells was investigated by a wound healing assay. MDA-MB-231 cells were seeded in a 12-well plate and grown overnight to confluence. The monolayer cells were scored with a 10 μL pipette tip to make a straight wound, and cells were washed with L15 medium to remove cell debris and then incubated with L15 medium without serum. Then cells were incubated with compound **5** in varied concentration for 48 h. Cell migration into the wound surface was photographed under phase contrast microscopy (Olympus) at 0, 24, and 48 h, respectively.

4.5. Chemistry

The in-house Natural Product Database (NPD) is our in-house collection of 4000 natural products isolated from more than 50 plants and their structures, which were established by extensive spectroscopy. The purity of all compounds was checked using NMR and HPLC and the minimum purity of all compounds is 95%. The detailed data of the natural products as mentioned above in the report are listed as follows.

4.5.1. Compound 1

Methyl rosmarinate, isolated from *Dracocephalum forrestii*; yellow powder; ESI-MS: *m/z* 397 $[M+Na]^+$; ^1H NMR (600 MHz, CD_3OD, δ): 6.68 (br s, 1H), 6.70 (d, 1H, J = 7.8 Hz), 6.57 (dd, 1H, J = 1.8, 7.8 Hz), 3.02 (m, 1H), 3.38 (m, 1H), 5.19 (t, 1H, J = 5.4 Hz), 7.04 (br s, 1H), 6.77 (d, 1H, J = 7.8 Hz), 6.95 (dd, 1H, J = 1.8, 7.8 Hz), 7.54 (d, 1H, J = 16.0 Hz), 6.25 (d, 1H, J = 16.0 Hz), 3.69 (s, 3H); ^{13}C NMR (150 MHz, CD_3OD, δ): 128.8, 116.3, 147.9, 145.4, 117.5, 121.8, 37.9, 74.7, 172.2, 127.6, 114.2, 146.2, 149.8, 116.5, 123.2, 146.8, 115.3, 168.3, 52.7.

4.5.2. Compound 2

Macrathoin F, isolated from *Ainsliaea macrocephala* (Mattf.) Y.C. Tseng; yellow powder; ESI-MS: *m/z* 529 $[M-H]^-$; ^1H NMR (300 MHz, CD_3OD, δ): 7.61 (d, 1H, J = 15.9 Hz), 7.50 (d, 1H, J = 15.9 Hz), 7.04 (d, 1H, J = 1.8 Hz), 7.00 (d, 1H, J = 1.8 Hz), 6.91 (dd, 2H, J = 1.8, 8.4 Hz), 6.75 (d, 2H, J = 8.4 Hz), 6.28 (d, 1H, J = 15.9 Hz), 6.16 (d, 1H, J = 15.9 Hz), 5.55 (m, 1H), 5.11 (dd, 1H, J = 3.0, 8.1 Hz), 4.33 (m, 1H), 3.71 (s, 3H), 2.26 (m, 4H); ^{13}C NMR (75 MHz, CD_3OD, δ): 75.8, 38.4, 69.1, 74.9, 68.6, 175.2, 127.6, 127.7, 115.2, 146.8, 149.7, 116.5, 123.1, 147.7, 114.6, 114.7, 167.9, 168.5, 53.1.

4.5.3. Compound 3

Methy-3-*O*-caffeoylquinate, isolated from *Ainsliaea macrocephala* (Mattf.) Y.C. Tseng; white powder; ESI-MS: *m/z* 367 $[M-H]^-$; ^1H NMR (300 MHz, CD_3OD, δ): 7.53 (d, 1H, J = 15.9 Hz), 7.04 (d, 1H, J = 2.1 Hz), 6.96 (dd, 1H, J = 2.1, 8.1 Hz), 6.88 (d, 1H, J = 8.1 Hz), 6.22 (d, 1H, J = 15.9 Hz), 5.27 (m, 1H), 4.12 (m, 1H), 3.75 (m, 1H), 3.70 (s, 3H), 2.02∼2.25 (m, 4H); ^{13}C NMR (75 MHz, CD_3OD, δ): 75.8, 37.8, 72.5, 70.3, 71.8, 37.8, 175.4, 127.7, 115.7, 149.7, 146.9, 115.7, 122.8, 146.2, 118.6, 168.3, 52.8.

4.5.4. Compound 4

(+)-2-(1-Hydroxyl-4-oxocyclohexyl) ethyl caffeate, isolated from *Incarvillea Mairei* var. *Grandiflora*; brown solid; ESI-MS: *m/z* 343 $[M+Na]^+$; ^1H NMR (600 MHz, CD_3OD, δ): 7.48 (1H, s), 6.79 (1H, d, J = 8.0 Hz), 6.94 (1H, d, J = 8.0 Hz), 7.60 (1H, d, J = 15.0 Hz), 6.25 (1H, d, J = 15.0 Hz), 2.05 (2H, m), 1.04–1.91 (3H, m), 2.70 (2H, m), 2.22 (2H, d, J = 15.0 Hz), 1.98 (1H, t, J = 7.0 Hz), 4.38 (1H, t, J = 7.0 Hz), 4.33 (1H, m); ^{13}C NMR (150 MHz, CD_3OD, δ): 127.6, 115.1, 146.6, 149.4, 116.4, 122.8, 146.8, 115.2, 169.2, 69.8, 37.7, 37.6, 214.5, 41.3, 61.7.

4.5.5. Compound 5

Dimethyl lithospermate, isolated from *Dracocephalum forrestii*; yellow powder; ESI-MS: *m/z* 598 $[M+Na]^+$; ^1H NMR (600 MHz, CD_3OD, δ): 6.71 (dd, 1H, J = 1.8, 7.8 Hz), 7.19 (d, 1H, J = 1.8 Hz), 7.73 (d, 1H, J = 16.2 Hz), 6.30 (d, 1H, J = 16.2 Hz), 6.79 (d, 1H, J = 1.8 Hz), 6.76 (d, 1H, J = 7.8 Hz), 6.82 (d, 1H, J = 7.8 Hz), 5.90 (d, 1H, J = 4.8 Hz), 4.43 (d, 1H, J = 4.8 Hz), 6.71 (d, 1H, J = 1.8 Hz), 6.69 (d, 1H, J = 7.8 Hz), 6.58 (dd, 1H, J = 1.8, 7.8 Hz), 3.00(m, 2H), 5.19 (dd, 1H, J = 4.8, 8.4 Hz), 3.70 (s, 3H), 3.71 (s, 3H). ^{13}C NMR (150 MHz, CD_3OD, δ): 124.4, 127.0, 148.8, 146.8, 118.4, 121.8, 144.1, 116.3, 168.0, 133.4, 113.5, 146.2, 145.3, 116.3, 118.4, 88.5, 57.3, 173.6, 128.7, 117.5, 146.6, 145.3, 116.4, 122.0, 37.8, 74.7, 172.1, 52.7, 53.2.

4.5.6. Compound 6

9′-*O*-*n*-Butyl lithospermate, isolated from *Dracocephalum forrestii*; yellow powder; ESI-MS: *m/z* 617 $[M+Na]^+$; ^1H NMR (600 MHz, CD_3OD, δ): 6.82 (d, 1H, J = 8.1 Hz), 7.17 (d, 1H, J = 8.1 Hz), 7.72 (d, 1H, J = 15.6 Hz), 6.30 (d, 1H, J = 15.6 Hz), 6.79 (d, 1H, J = 1.8 Hz), 6.77 (d, 1H, J = 8.1 Hz), 6.71 (dd, 1H, J =1.8, 8.1 Hz), 5.90 (d, 1H, J = 4.2 Hz), 4.42 (d, 1H, J = 4.8 Hz), 6.76 (d, 1H, J = 1.8 Hz), 6.69 (d, 1H, J = 7.8 Hz), 6.63 (dd, 1H, J = 1.8, 7.8 Hz), 2.97 (dd, 1H, J = 9.0, 14.0 Hz), 3.09 (dd, 1H, J = 3.6, 14.4 Hz), 5.14 (dd, 1H, J = 3.6, 9.0 Hz), 4.09 (dd, 2H, J = 1.8, 8.4 Hz), 1.48 (m, 2H), 1.22 (m, 2H), 0.86 (t, 3H, J = 7.2 Hz). ^{13}C NMR (150 MHz, CD_3OD, δ): 123.8, 126.1, 147.9, 144.2, 117.5, 120.9, 143.0, 115.9, 167.4, 132.6, 112.6, 145.2, 145.9, 115.6, 117.5, 87.5, 56.5, 172.3, 129.0, 116.6, 145.7, 144.3, 115.4, 121.0, 37.3, 75.0, 174.1, 66.0, 30.7, 19.2, 13.1.

4.5.7. Compound 7

Isoacteoside, isolated from *Incarvillea delavayi* Bur. et Franch.; yellow amorphous powder; ESI-MS: *m/z* 647 $[M+Na]^+$; ^1H NMR (300 MHz, CD_3OD, δ): 7.58 (d, 1H, J = 15.6 Hz), 6.54-7.06 (6H, aromatic H), 6.31(d, 1H, J = 15.9 Hz), 5.21 (s, 1H), 4.35 (d, 1H, J = 7.5 Hz), 2.79 (t, 2H, J = 7.5 Hz), 1.26 (d, 3H, J = 6.0 Hz), ^{13}C NMR (75 MHz, CD_3OD, δ): Aglycone moiety: 131.3, 116.3, 144.6, 146.1, 117.1, 121.3, 72.4, 36.6; Caffeoyl moiety: 127.6, 114.8, 149.6, 146.7, 116.5, 123.2, 169.1, 115.1, 147.2; Glucose moiety: 104.3, 75.3, 83.9, 70.0, 75.6, 64.6; Rhamnose moiety: 102.7, 72.3, 72.2, 74.0, 70.3, 17.9.

4.5.8. Compound 8

Quercetin, isolated from *Hypericum japonicum* Thunb. ex Murray; yellow needle crystal; EI-MS: *m/z* 302 $[M]^+$; ^1H NMR (500 MHz, DMSO-d_6, δ): 7.69 (d, 1H, J = 2 Hz), 6.92 (dd, 1H, J = 8, 2 Hz), 6.89 (d, 1H, J = 9 Hz), 6.42 (d, 1H, J = 2 Hz), 6.20 (d, 1H, J = 2 Hz), 12.49 (-OH), 10.80 (–OH), 9.60 (–OH), 9.35 (–OH), 9.35 (–OH); ^{13}C NMR (125 MHz, DMSO-d_6, δ): 175.8, 163.8, 160.7, 156.1, 147.7, 146.8, 145.0, 135.7, 121.9, 119.9, 115.6, 115.0, 102.9, 98.1, 93.3.

4.5.9. Compound 9

Luteolin, isolated from *Dracocephalum forrestii*; yellow crystal; ESI-MS: *m/z* 309 $[M+Na]^+$; ^1H NMR (600 MHz, CD_3OD, δ): 6.52 (s, 1H), 6.20 (d, 1H, J = 1.8 Hz), 6.43 (d, 1H, J = 1.8 Hz), 7.37 (d, 1H, J = 2.4 Hz), 6.89 (d, 1H, J = 9.0 Hz), 7.37 (dd, 1H, J = 2.4, 9.0 Hz); ^{13}C NMR (150 MHz, CD_3OD, δ): 166.0, 103.9, 183.9, 163.2, 100.1, 166.4, 95.0, 159.4, 105.3, 123.7, 114.2, 147.0, 151.0, 116.8, 120.3.

4.5.10. Compound 10

Daphnodorin F, isolated from *Daphne odora* Thunb. *var. actrocaulis* Rehd.; yellow powder; ESI-MS: *m/z* 565 $[M+Na]^+$; ^1H NMR (500 MHz, CD_3OD, δ): 1.92 and 2.21 (2 m, 2H), 2.72 (m, 2H), 4.82 (d, 2H, J = 7 Hz), 5.83 (d, 1H, J = 2 Hz), 5.91 (d, 1H, J = 2 Hz), 6.19 (s, 1H), 6.74 (d, 2H, J = 9 Hz), 6.79 (d, 2H, J = 8 Hz), 7.06 (d, 2H, J = 8 Hz), 7.31 (2H, d, J = 9 Hz). 13C NMR (125 MHz, CD_3OD, δ): 20.3, 30.7, 78.5, 82.6, 91.9, 95.6, 97.3, 100.2, 105.4, 107.6, 115.6, 115.9, 118.8, 126.4, 127.8, 129.4, 133.9, 154.2, 157.6, 159.7, 159.8, 161.1, 163.2, 165.2, 168.6, 194.2

4.5.11. Compound 11

Dihydrodaphnodorin B, isolated from *Daphne holosericea* (Diels) Hamaya; yellow oily liquid; ESI-MS: *m/z* 543 $[M-H]^-$; ^1H NMR (300 MHz, DMSO-d_6, δ): 2.47 (dd, 1H, J = 7.2, 17.4 Hz), 2.56 (dd, 1H, J = 4.8, 16.2 Hz), 3.76 (br s, 1H), 4.70 (d, 1H, J = 6.0 Hz), 5.03 (d, 1H, J = 4.2 Hz), 6.01 (s, 1H), 5.81 (d, 1H, J = 10.2 Hz), 6.03 (d, 1H, J = 10.2 Hz), 6.61 (d, 2H, J = 9.0 Hz), 6.54 (d, 2H, J = 9.0 Hz), 6.98 (d, 2H, J = 8.4 Hz), 7.02 (d, 2H, J = 8.4 Hz), 9.29 (s, 1H), 9.37 (s, 1H), 10.28 (s, 1H), 10.86 (s, 1H), 13.56 (s, 1H); ^{13}C NMR (150 MHz, DMSO-d_6, δ): 80.3, 66.9, 27.0, 164.7, 89.1, 104.8, 160.0, 99.9, 128.6, 127.4, 114.3, 156.7, 87.1, 55.3, 201.4, 156.6, 94.6, 156.4, 104.1, 130.2, 128.2, 114.7, 150.7.

4.5.12. Compound 12

(2*R*,3*S*)-Dihydromyricetin, isolated from *Rhododendron spinuliferum* Franch.; white powder; ESI-MS: *m/z* 321 $[M+H]^+$; ^1H NMR (500 MHz, CD_3OD, δ): 4.54 (1H, d, J = 12.0 Hz, H-3), 4.93 (1H, d, J = 11.0 Hz, H-2), 6.58 (2H, s, H-2′, 6′); ^{13}C NMR (125 MHz, CD_3OD, δ): 73.6, 85.2, 96.3, 97.3, 101.8, 107.7, 108.1, 129.1, 134.8, 146.8, 164.4, 165.2, 168.6, 198.2.

4.5.13. Compound 13

Dihydroquercetin, isolated from *Abies georgei* Orr.; amorphous powder; ESI-MS: *m/z* 327 $[M+Na]^+$, 631 $[2M+Na]^+$; ^1H NMR (600 MHz, CD_3OD, δ): 4.90 (d, 1H, J = 11.7 Hz), 4.52 (d, 1H, J = 11.7 Hz), 5.92 (s, 1H), 5.88 (s, 1H), 6.98 (d, 1H, J = 8.1 Hz), 6.82 (d, 1H, J = 8.1 Hz), 7.00 (s, 1H); ^{13}C NMR (150 MHz, CD_3OD, δ): 84.9, 73.5, 198.4, 165.0, 97.4, 168.7, 96.4, 164.4, 101.7, 129.7, 121.0, 116.1, 146.1, 146.9, 115.9.

4.5.14. Compound 14

1,3,6,7-Tetrahydroxyxanthonin, isolated from *Hypericum japonicum* Thunb. ex Murray; yellow crystal; ESI-MS: *m/z* 260 $[M]^+$; ^1H NMR (500 MHz, DMSO-d_6, δ): 6.15 (d, 1H, 2 Hz), 6.32 (d, 1H, 2 Hz), 6.84 (s, 1H), 7.37 (s, 1H). ^{13}C NMR (125 MHz, DMSO-d_6, δ): 162.6, 97.6, 164.6, 93.6, 157.3, 151.1, 102.5, 154.7, 143.9, 107.8, 111.5, 178.8, 101.5.

4.5.15. Compound 15

(−)-Secoisolariciresinol, isolated from *Daphne bholua* Buch. -Ham.; white crystal; ESI-MS: *m/z* 385 $[M+Na]^+$; ^1H NMR (500 MHz, DMSO-d_6, δ): 6.64 (2H, d, J = 1.0 Hz), 6.61 (1H, d, J = 8.0 Hz), 6.49 (1H, dd, J = 1.0, 8.0 Hz), 2.50 (4H, m), 1.80 (2H, br s), 3.36 (4H, m), 3.67 (6H, s); ^{13}C NMR (125 MHz, DMSO-d_6, δ): 132.3, 113.0, 147.3, 144.3, 115.1, 121.2, 34.0, 42.5, 60.3, 55.5.

4.5.16. Compound 16

(−)-Threo-guaiacylglycerol-8-*O*-4′-(coniferyl alcohol) ether, isolated from *Brucea javanica* L. Merr; Brown powder; ESI-MS: *m/z* 399 $[M+Na]^+$; ^1H NMR (500 MHz, DMSO-d_6, δ): 1.13 (1H, d, J = 2.0 Hz), 6.83 (1H, d, J = 8.0 Hz), 6.88 (1H, dd, J = 8.0, 2.0 Hz), 4.28 (1H, m), 4.20 (2H, dd, J = 5.0, 1.0 Hz), 7.00 (1H, d, J = 2.0 Hz), 6.48 (1H, d, J = 8.0 Hz), 6.91 (1H, dd, J = 8.0, 2.0 Hz), 7.32 (1H, d, J = 16.0 Hz), 6.53 (1H, dd, J = 16.0, 8.0 Hz), 3.81 (3H, s), 3.88(3H, s). ^{13}C NMR (125 MHz, DMSO-d_6, δ): 133.8, 111.8, 148.9, 147.2, 115.9, 120.8, 74.1, 87.2, 61.9, 133.2, 111.3, 151.8, 149.2, 118.9, 120.8, 128.7, 131.4, 63.8, 56.4, 56.6.

4.5.17. Compound 17

8(14)-Podocarpen-13-on-18-oic acid, isolated from *Abies georgei* Orr.; amorphous powder; ESI-MS: *m/z* 299 $[M+Na]^+$; ^1H NMR (300 MHz, CD_3OD, δ): 0.86 (3H, s), 1.20 (3H, s), 2.15 (1H, dd,

J = 12.3, 2.7 Hz), 2.50 (1H, dd, J = 10.5, 3.6 Hz), 5.85 (1H, br s); ^{13}C NMR (75 MHz, CD_3OD, δ): 39.6, 19.2, 38.3, 48.3, 49.4, 25.3, 36.4, 169.3, 53.0, 39.5, 21.4, 37.5, 202.6, 126.4, 183.5, 17.9, 15.9.

4.5.18. Compound 18

Oxyresveratrol, isolated from *Veratrum dahuricum*; white amorphous powder; ESI-MS: m/z 245 $[M+H]^+$; ^{1}H NMR (600 MHz, CD_3OD, δ): 6.53 (d, 3H, J = 1.8 Hz), 6.28 (d, 1H, J = 1.8 Hz), 6.50 (dd, 1H, J = 8.4, 2.4 Hz), 7.40 (d, 1H, J = 8.4 Hz), 6.84 (d, 1H, J = 16.2 Hz), 7.10 (d, 1H, J = 16.2 Hz).

4.5.19. Compound 19

α-Isovaleroxyisovaleric acid, isolated from *Valeriana jatamansi* Jones; Colorless oily liquid; ESI-MS: m/z 225 $[M+Na]^+$; ^{1}H NMR (300 MHz, $CDCl_3$, δ): 4.88 (1H, d, J = 4.5 Hz), 2.29 (1H, m), 1.02 (6H, d, J = 6.6 Hz), 2.31 (2H, m), 2.16 (1H, m), 0.98 (6H, d, J = 6.6 Hz); ^{13}C NMR (75 MHz, CDCl3, δ): 77.0, 30.0, 18.8, 17.2, 173.2, 43.1, 25.7, 22.4

Acknowledgments

This work was supported by the Innovation Program of Shanghai Municipal Education Commission (Grant 10ZZ41), the National Natural Science Foundation of China (Grants 21173076, 81102375 and 10979072), the Specialized Research Fund for the Doctoral Program of Higher Education of China (Grants 20090074120012 and 20110074120009), the 111 Project (Grant B07023), the Shanghai Committee of Science and Technology (Grants 11DZ2260600, 10431902600 and 09dZ1975700), the Fundamental Research Funds for the Central Universities, the 863 Hi-Tech Program of China (Grant 2012AA020308), the Special Fund for Major State Basic Research Project (Grant 2009CB918501), and the National S&T Major Project of China (Grant 2011ZX09307-002-03). H.L. is also sponsored by Shanghai Rising-Star Program (Grant 10QA1401800) and Program for New Century Excellent Talents in University (Grant NCET-10-0378). The MMP-1 expression plasmid was kindly provided by Professor Zigang Dong (University of Minnesota). The MMP-12 expression plasmid was kindly provided by Dr. Herbert Nar (Boehringer Ingelheim Pharma KG), The MMP-2 and MMP-9 plasmids were kindly provided by Dr. William G. Stetler-Stevenson (NCI, National Institutes of Health). The MMP-3 and MMP-13 plasmids were kindly provided by Professor Christopher M. Overall (University of British Columbia).

References and notes

1. Marques, S. M.; Nuti, E.; Rossello, A.; Supuran, C. T.; Tuccinardi, T.; Martinelli, A.; Santos, M. A. *J. Med. Chem.* **2008**, *51*, 7968.
2. Yoon, S. O.; Park, S. J.; Yun, C. H.; Chung, A. S. *J. Biochem. Mol. Biol.* **2003**, *36*, 128.
3. Mannello, F.; Tonti, G.; Papa, S. *Curr. Cancer Drug Targets* **2005**, *5*, 285.
4. Fingleton, B. *Expert Opin. Ther. Targets* **2003**, *7*, 385.
5. Overall, C. M.; Kleifeld, O. *Nat. Rev. Cancer* **2006**, *6*, 227.
6. Martin, M. D.; Matrisian, L. M. *Cancer Metastasis Rev.* **2007**, *26*, 717.
7. Whittaker, M.; Floyd, C. D.; Brown, P.; Gearing, A. J. *Chem. Rev.* **2001**, *101*, 2205.
8. Mannello, F. *Recent Patents Anti-Cancer* **2006**, *1*, 91.
9. Harvey, A. *Drug Discovery Today* **2000**, *5*, 294.
10. Bukowski, R. M. *Expert Opin. Investig. Drugs* **2003**, *12*, 1403.
11. Weber, M. H.; Lee, J.; Orr, F. W. *Int. J. Oncol.* **2002**, *20*, 299.
12. Latreille, J.; Batist, G.; Laberge, F.; Champagne, P.; Croteau, D.; Falardeau, P.; Levinton, C.; Hariton, C.; Evans, W. K.; Dupont, E. *Clin. Lung Cancer* **2003**, *4*, 231.
13. Kousidou, O. C.; Mitropoulou, T. N.; Roussidis, A. E.; Kletsas, D.; Theocharis, A. D.; Karamanos, N. K. *Int. J. Oncol.* **2005**, *26*, 1101.
14. Stahl, M.; Guba, W.; Kansy, M. *Drug Discovery Today* **2006**, *11*, 326.
15. Lyne, P. D. *Drug Discovery Today* **2002**, *7*, 1047.
16. Rollinger, J. M.; Stuppner, H.; Langer, T. *Prog. Drug Res.* **2008**, *65*(211), 213.
17. Wang, J. L.; Liu, D. X.; Zhang, Z. J.; Shan, S. M.; Han, X. B.; Srinivasula, S. M.; Croce, C. M.; Alnemri, E. S.; Huang, Z. W. *Proc. Natl. Acad. Sci. U.S.A.* **2000**, *97*, 7124.
18. Yang, S. M.; Scannevin, R. H.; Wang, B.; Burke, S. L.; Wilson, L. J.; Karnachi, P.; Rhodes, K. J.; Lagu, B.; Murray, W. V. *Bioorg. Med. Chem. Lett.* **2008**, *18*, 1135.
19. Pirard, B. *Drug Discovery Today* **2007**, *12*, 640.
20. Terp, G. E.; Cruciani, G.; Christensen, I. T.; Jorgensen, F. S. *J. Med. Chem.* **2002**, *45*, 2675.
21. Kallblad, P.; Todorov, N. P.; Willems, H. M.; Alberts, I. L. *J. Med. Chem.* **2004**, *47*, 2761.
22. Pirard, B.; Matter, H. *J. Med. Chem.* **2006**, *49*, 51.
23. Pochetti, G.; Montanari, R.; Gege, C.; Chevrier, C.; Taveras, A. G.; Mazza, F. *J. Med. Chem.* **2009**, *52*, 1040.
24. DeLano, W. 2002, http://www.pymol.org.
25. Stierand, K.; Maass, P. C.; Rarey, M. *Bioinformatics* **2006**, *22*, 1710.